
ORIGINAL ARTICLE

Computational Identification of TNNC1-Binding Compounds for
The Therapeutic Modulation of Cardiomyopathy

N. Ravi, U. S. H. Raghavendra Prasad, N. Sravanthi, * M. Kavitha

Department of Chemistry, University College of Science, Osmania University, Hyderabad 500007,
Telangana, India

*Corresponding author's email: kavithamannem@gmail.com; kavithamannem@osmania.ac.in

ABSTRACT

Cardiomyopathy encompasses a diverse group of myocardial disorders that compromise the structural and functional integrity of the heart muscle, often leading to impaired contractility, arrhythmias, and progression to heart failure. Among the various genetic contributors, mutations in the TNNC1 gene which encodes cardiac troponin C, a key calcium-binding component of the troponin complex have been implicated in both hypertrophic and dilated cardiomyopathy. TNNC1 plays a crucial role in regulating myocardial contraction through calcium-mediated signaling. Alterations in its function can disrupt calcium sensitivity and sarcomeric dynamics, contributing to abnormal cardiac remodeling and clinical deterioration. Understanding TNNC1-associated cardiomyopathy offers valuable insights into genotype-phenotype correlations and paves the way for precision-targeted therapeutic strategies. In this study, computational methods were employed to screen and identify candidate inhibitors targeting cardiomyopathy.

Keywords: *Cardiomyopathy, TNNC1 gene, cardiac remodeling, sarcomeric dynamics*

Received 21.05.2025

Revised 24.06.2025

Accepted 10.07.2025

How to cite this article:

N. Ravi, U. S. H. Raghavendra Prasad, N. Sravanthi, M. Kavitha. Computational Identification of TNNC1-Binding Compounds for The Therapeutic Modulation of Cardiomyopathy. Adv. Biores. Vol 16 [4] July 2025.33-44

INTRODUCTION

Cardiomyopathy refers to a group of structural and functional disorders of the myocardium that impair the heart's ability to pump blood efficiently [1-5]. It encompasses various subtypes, including dilated, hypertrophic, and restrictive forms, each characterized by distinct pathological features and clinical outcomes [6,7]. These conditions may arise due to genetic mutations, chronic hypertension, metabolic disorders, or infections, and often progress to heart failure, arrhythmias, or sudden cardiac death. Understanding molecular mechanisms and genetic basis of cardiomyopathy is essential for improving early diagnosis, risk stratification, and targeted therapeutic strategies [8,9].

Biochemical Pathway

Mutations in the TNNC1 gene, encoding cardiac troponin C, disrupt calcium-binding affinity and impair the function of the troponin complex [10]. These alterations compromise myofibrillar interactions and cardiac muscle contraction, leading to defective calcium regulation. Consequently, these molecular dysfunctions contribute to the onset and progression of cardiomyopathy [11]. This pathway elucidates the biochemical cascade from gene mutation to clinical pathology.

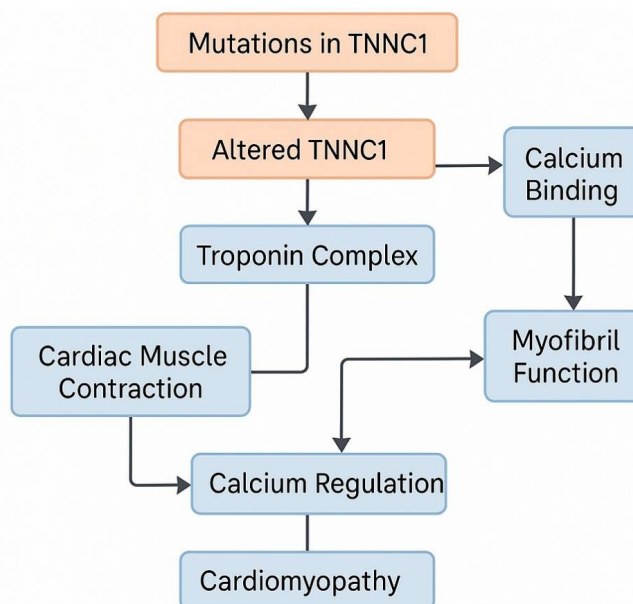


Figure 1. Explains the Molecular cascade of Cardiomyopathy

MATERIAL AND METHODS

Retrieval of Protein biological information and 3D structure

The UniProt database serves as a fundamental resource in bioinformatics, providing a comprehensive and well-curated repository of protein sequences along with associated annotations [12]. It is extensively utilized in various fields of biological research and integrates data from trusted sources, including Swiss-Prot, TrEMBL, and PIR. UniProt delivers detailed information on protein functions, sequence properties, structural attributes, and taxonomic classification.

The Protein Data Bank (PDB) is a publicly accessible digital archive that houses three-dimensional structural information of biological macromolecules, including proteins, nucleic acids, and their complexes [13]. It features structural data contributed by scientists globally, derived mainly from experimental methods like X-ray crystallography, nuclear magnetic resonance (NMR) spectroscopy, and cryo-electron microscopy. PDB plays a crucial role in advancing structural biology, facilitating drug discovery, and supporting computational modeling efforts.

Validation

The three-dimensional model of TNNC1 was evaluated for stereochemical quality using the PROCHECK [14] tool, available through the SAVES (Structural Analysis and Verification Server) platform [15]. To further validate the structure, a Ramachandran plot was generated to examine the distribution of backbone dihedral angles relative to amino acid residues [16, 17]. The structural integrity and accuracy were also assessed by comparing sequence-to-structure alignment and analyzing stability using energy-based metrics, including the Z-score provided by the ProSA program, which benchmarks the model against experimentally determined protein structures [18].

Structure-based virtual screening using molecular docking

Molecular docking is a computational technique employed to simulate the interaction between small molecules and target proteins, playing a crucial role in drug discovery and lead optimization [19]. It aims to discover new chemical compounds that can bind efficiently to specific protein sites, potentially triggering the desired biological effect. The effectiveness of virtual screening is closely linked to a thorough knowledge of the protein's structural characteristics and energy profile [20].

Docking is an essential method in structure-based drug design [21], used to investigate different ligand conformations and predict how they interact within the binding sites of target proteins. One widely used tool for this process is GLIDE (Grid-Based Ligand Docking with Energetics), which accurately predicts ligand binding orientations and estimates their affinity [22]. It utilizes a multi-step hierarchical screening process that analyzes the active site of the protein to identify optimal ligand interactions.

In this study, a structurally refined model of the TNNC1 protein was subjected to structure-based virtual screening using GLIDE. The Vander Waals parameters were adjusted with a scaling factor of 1.0 and a partial charge cutoff value of 0.25. A docking grid of dimensions X A0x YA0x Z A0 was constructed to encompass the binding site of interest. Ligands for docking were sourced from the Comprehensive Marine Natural Products Database (CMNPD) library [23]. These compounds were converted into three-dimensional structures at a physiological pH of 7.0 ± 2.0 using the LigPrep module within Maestro

(Schrodinger, LLC, New York), applying the OPLS_2004 force field [24]. Tautomer's, ionization states, and stereoisomers were generated using default parameters to ensure energetically favorable conformations. Following ligand preparation, compounds with the most favorable energy profiles underwent flexible docking targeting the predicted active site of the TNNC1 protein. This was executed through a stepwise protocol within the GLIDE module. Initially, High Throughput Virtual Screening (HTVS) mode was used to rapidly screen and eliminate less promising candidates. The top 10% of hits were then subjected to Standard Precision (SP) docking for more accurate evaluation. Subsequently, the highest-ranking ligands were further refined using Extra Precision (XP) mode to identify the most accurate binding conformations. After docking, the leading poses were optimized for bond geometry and rescored using the GLIDE Score function. The top candidates were then evaluated for pharmacokinetic suitability by analyzing their ADME [20] (Absorption, Distribution, Metabolism, and Excretion) properties.

ADMET

Evaluating the computational ADME (Absorption, Distribution, Metabolism, and Excretion) characteristics of ligand molecules offers critical insights into their potential as viable drug candidates [25]. This assessment plays a crucial role in the early phases of drug development, allowing researchers to identify and exclude compounds with poor pharmacokinetic behavior, thereby enhancing the likelihood of success in subsequent clinical trials.

Ligands with favorable Glide scores and energy profiles were further evaluated for their pharmacokinetic and physiochemical characteristics using the QikProp, a Schrödinger tool [26, 27]. This platform employs predicts absorption, distribution, and overall drug-likeness. Integrating these QikProp predictions with molecular docking data and in-depth structural analysis enabled the identification of promising lead compounds for targeting the TNNC1 protein.

The toxicity profile of the ligands calculated using online platform ProTox 3.0 on the cytochrome P450 enzyme. It gives information of each ligand is inhibits the enzyme activity or non-inhibitor of the enzyme.

RESULTS AND DISCUSSION

Retrieval of protein structures, followed by structural analysis and validation

Acquisition of protein structure

The three-dimensional crystal structure of TNNC1 was retrieved from the Protein Data bank (PDB) using the identifier 1J1D_A. The structure was chosen based on its high resolution (2.61 Å), completeness, and suitability for molecular docking studies. Prior to docking, the structure was prepared using Schrodinger software by eliminating water molecules, irrelevant chains, and heteroatoms. Additionally, polar hydrogen atoms were added, and Kollman charges were assigned to ensure the protein was properly configured for further computational analysis.

Validation of the TNNC1 Protein Model

To confirm the structural reliability of the TNNC1 protein model, a Ramachandran plot analysis was performed (Figure 2). This assessment demonstrated that 91.5% of the amino acid residues were situated within energetically favorable regions, reflecting a high degree of stereochemical correctness. In addition, the VERIFY_3D tool was utilized to evaluate the alignment between the linear amino acid sequence and the protein's three-dimensional environment [24]. Results revealed that 90 % of the 159 residues had a compatibility score above 0.2, supporting the model's structural soundness.

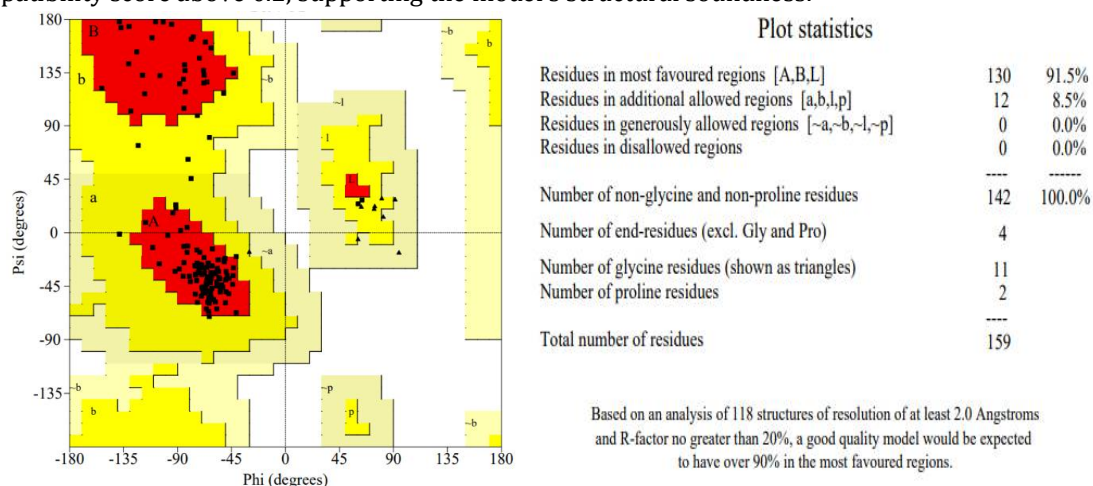


Figure 2: The Ramachandran Plot depicts stability of the protein TNNC1

Figure 2 The Ramachandran analysis revealed that 91.5% of residues were located in the most favorable conformational regions, which is considered indicative of a highly accurate and reliable model.

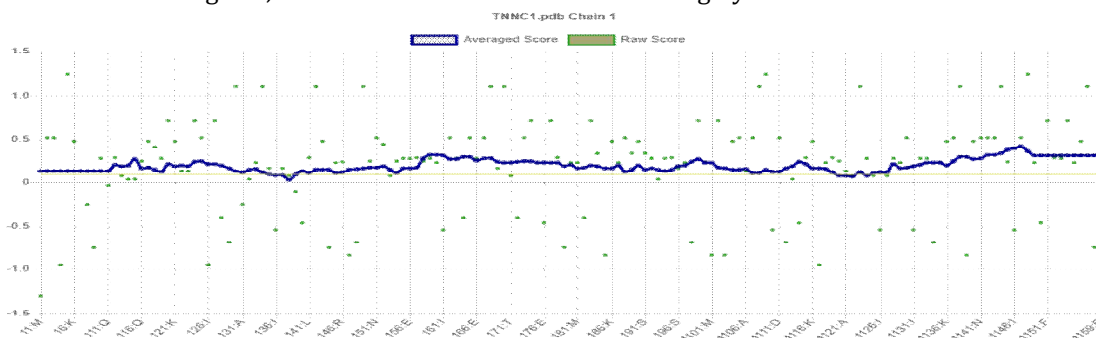


Figure 3: The Protein TNNC1 VERIFY_3D

The VERIFY_3D of the protein TNNC1 protein showing 90% of the protein had a compatibility score above 0.2. The ProSA-web server was also employed to evaluate global and local model quality (figure 3 and 4) [28]. By comparing the TNNC1 model to proteins of comparable size within the Protein Data Bank (PDB), the tool confirmed the model's validity.

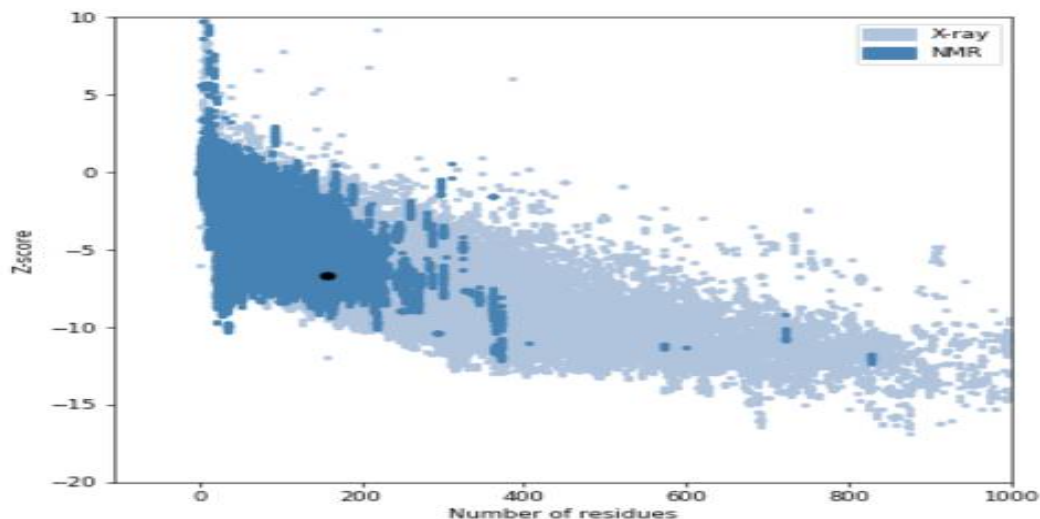


Figure 4: The determination of nativity of the protein TNNC1 using X-ray and NMR

The calculated Z-score from ProSA was -6.36, placing the TNNC1 model within the range typically observe for native protein structures obtained via experimental techniques such as X-ray crystallography and NMR spectroscopy.

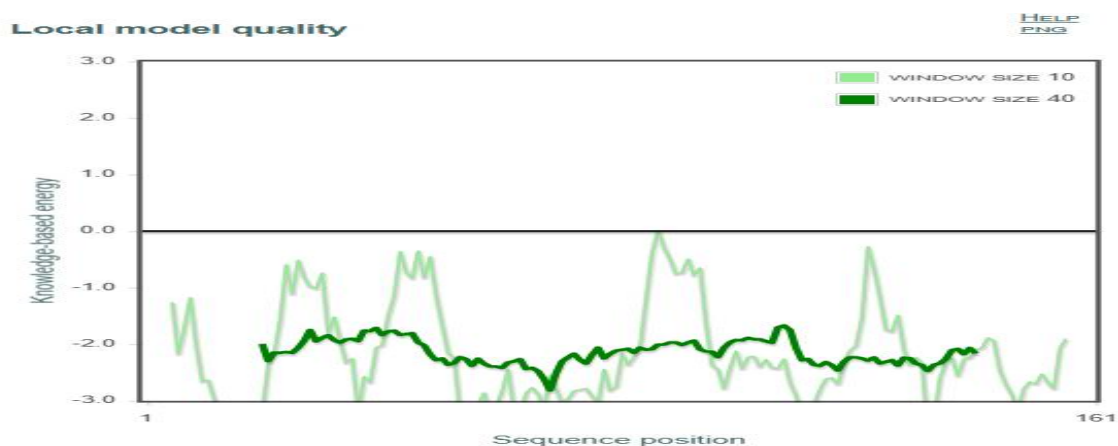


Figure 5 The model quality of the TNNC1

A knowledge-based energy plot using ProSA showed local model structural variations across the sequence (Figure 5). Energy values calculated over sliding windows (10 and 40 residues) mostly remained below the baseline, suggesting that the structure is locally stable.

Local Folding Pattern of the Protein TNNC1

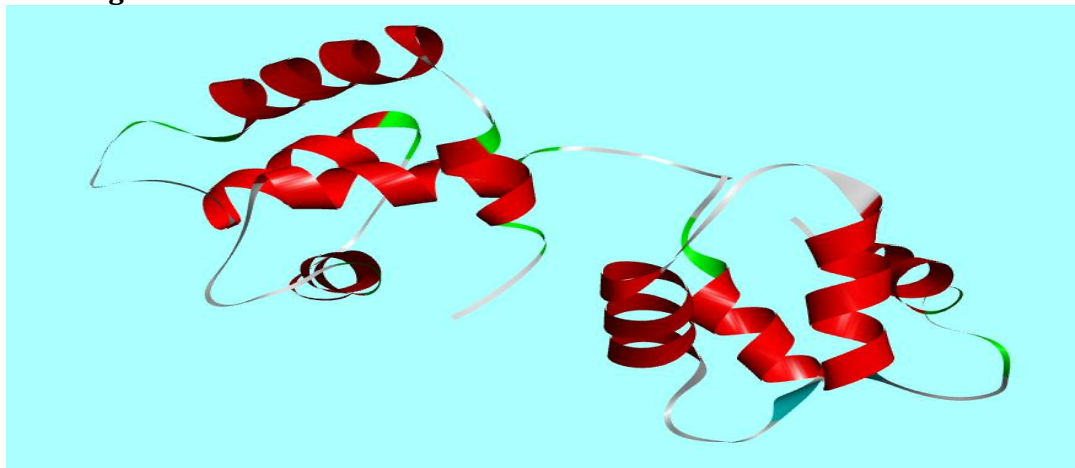


Figure 6: A 3D ribbon model of TNNC1 generated using using Accelrys studio shows the presence of α helices and β sheets

PDBsum analysis of the Protein TNNC1

Visual inspection and secondary structure analysis confirmed that TNNC1 contains α helices, β sheets. The PDBsum was used to generate a schematic view of these structural motifs, outlining their distribution throughout the protein (figure 7).

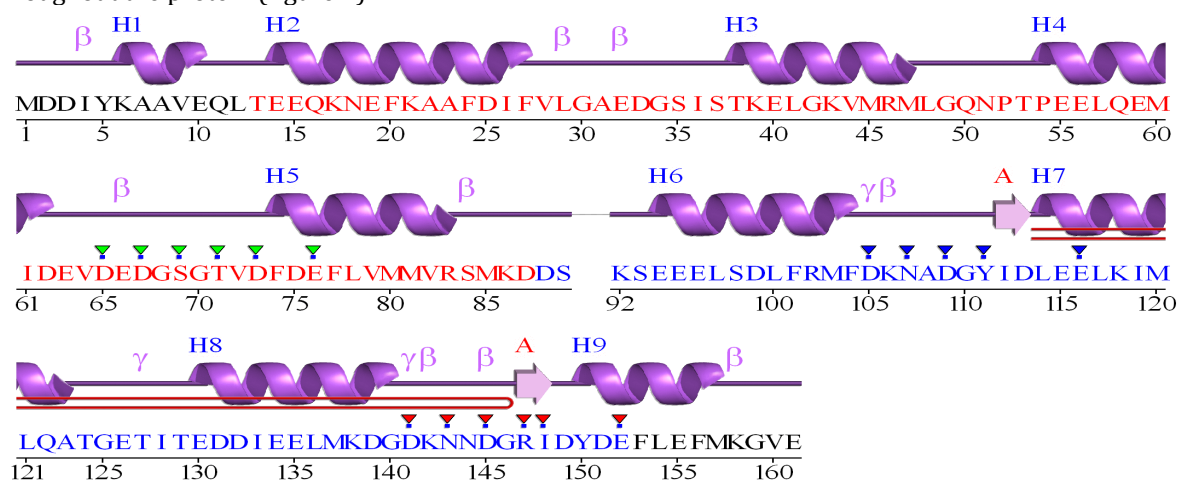


Figure 7: PDBsum Server prediction of Folding's in TNNC1

Figure 7 presents the secondary structure of the TNNC1 protein. It consists of 9 helices and 2 β sheets

Prediction of Active Sites Using Computational tools

To identify potential binding regions in TNNC1, computational approaches such as CASTp and SiteMap were employed [29-31]. CASTp utilized both Connolly's and Richards' surface models to locate four significant hydrophobic cavities (Table 1.), indicating likely interaction site for ligands or substrates.

Table 1: The Active sites assessment using CASTp and SiteMap

S.NO.	Active site predicting server/tool	Amino acids	Volume (Å)
1	CASTp	2,3,4,5,6,7,8,8,10,11,86,88,104,112,121,124,126,128,132,135,136,138,139,140,142,152,153,155,156,157,158,159,160,161	1141.690
2	SiteMap	4,5,7,8,11,12,16,82,83,85,86,87,88,89,92,159,160,161	215.061

The active site prediction using CASTp and SiteMap. Showing similar hydrophobic sites.

Among these, two prominent binding pockets were consistency identified by both CASTp and SiteMap. These sites correspond well with known protein-protein interaction regions, suggesting their relevance in the functional activity of TNNC1.

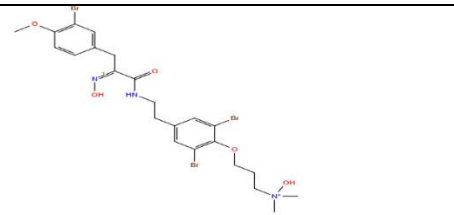
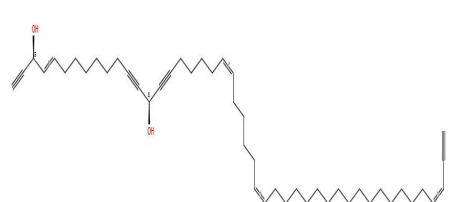
Virtual Screening and Molecular Docking

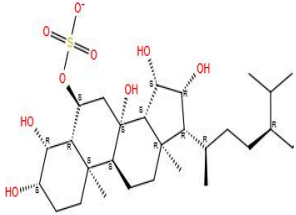
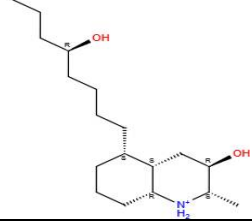
A structure-based virtual screening (SBVS) strategy was implemented to identify potential small-molecule binders targeting TNNC1 [32]. A 24.74 Å × 57.73 Å × 32.97 Å grid was defined over the predicted active site to enable docking. Ligands from the Comprehensive Marine Natural Products Database (CMNPD) were processed using Schrodinger's LigPrep module, which refined the geometries and considered multiple ionization and tautomeric states.

From an initial pool of 30,000 compounds, a total of 60,000 confirmers were generated. These subjected to multi-step docking using HTVS, SP and XP protocols in Glide. A total of 41 ligands exhibited strong binding affinities, and the top 5 were shortlisted based on Glide scores (Table 2).

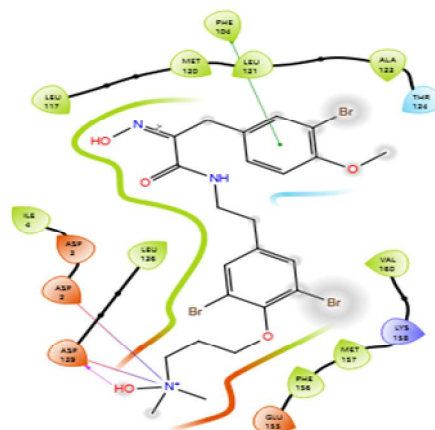
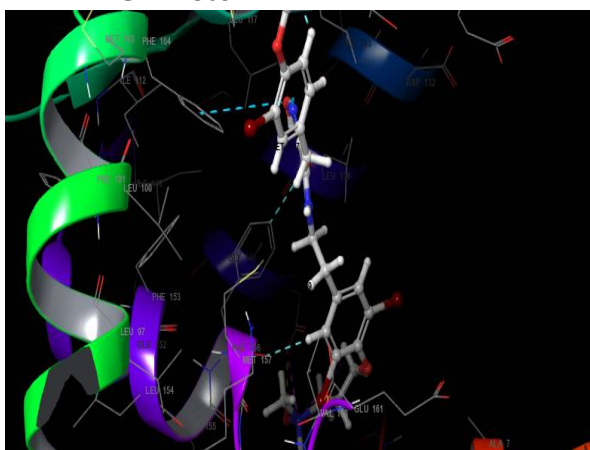
Hydrogen bond analysis revealed interactions with bond lengths ranging from 1.67 Å to 3.62 Å (Table 2) these interactions were further visualized using Accelrys Discovery Studio, confirming the stability and specificity of ligand binding to TNNC1 [33].

Table 2: Indicating the ligand- TNNC1 interactions

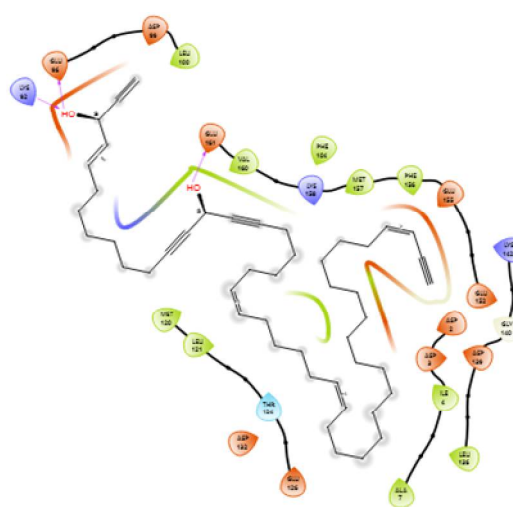
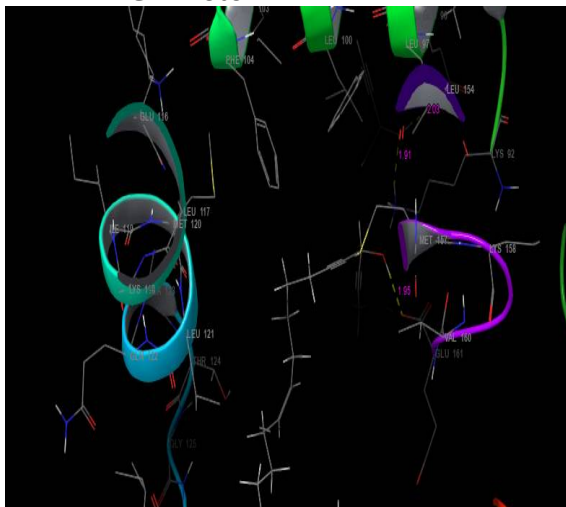
S. NO.	Ligand (D)	Glide Score	Glide Energy(kcal/mol)	H- Bond	H - bond Distances (Å)
D1		-8.715	-65.475	D1-ASP139 D1- ASP 139(A) D1- PHE 156(A) D1-MET 120 (A)	2.44 3.24 3.34 2.75
D2		-7.950	-63.52	D2 - GLU161 D2 - GLU96 D2- LYS92	1.95 2.03 1.91

D3		-7.556	-59.582	D3-ASP139 D3-ASP2 D3- LYS92 D3-LYS92(A)	1.81 2.38 2.60 2.99
D4		-6.982	-56.915	D4-ASP139 D4- ASP2 D4-ASP2(A)	1.83 1.81 3.28
D5		-6.728	-53.871	D5-ASP139 D5-ASP139 D5- ASP139(A) D5-ASP2(A) D5-ASP2(A)	1.80 1.67 3.23 3.60 3.62

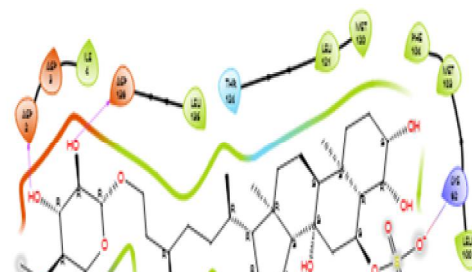
D1- TNNC1 Protein



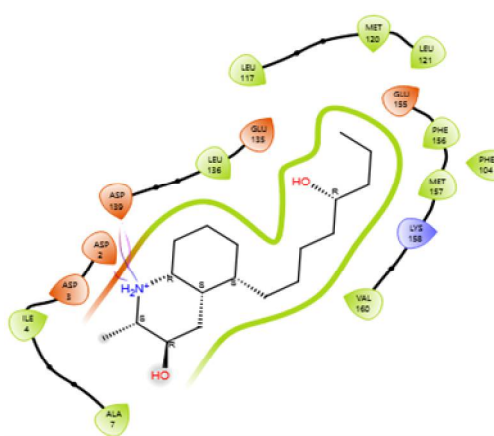
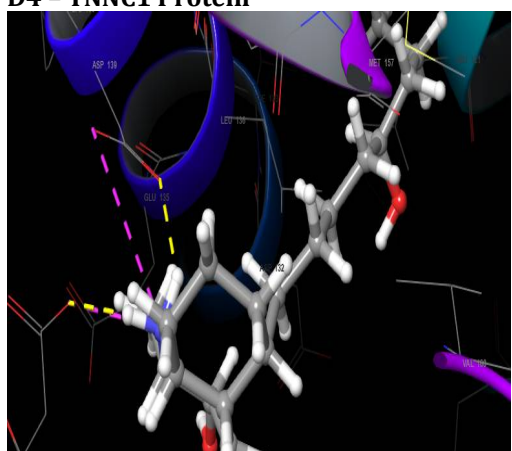
D2 - TNNC1 Protein



D3 - TNNC1 Protein



D4 - TNNC1 Protein



D5 - TNNC1 Protein

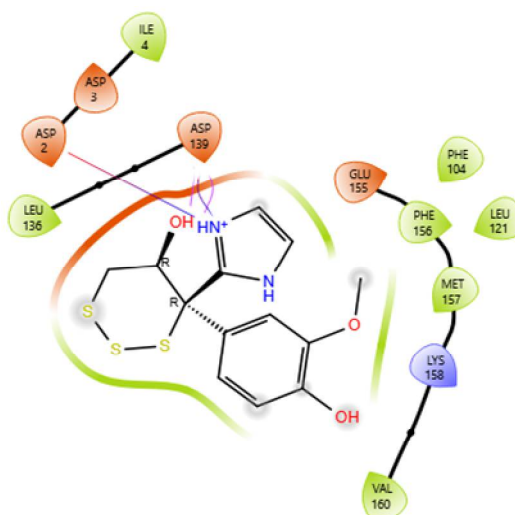
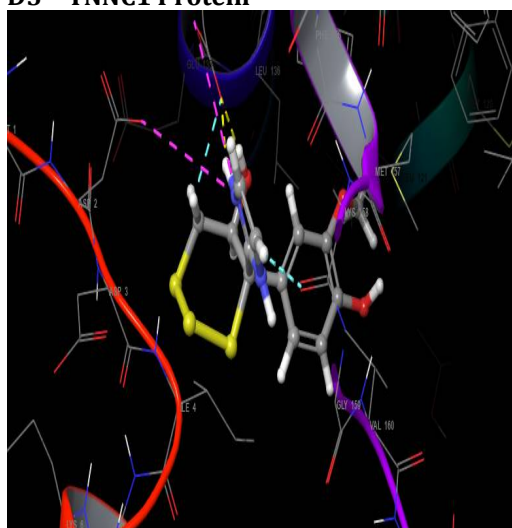


Figure 8: TNNC1- drug interactions shown in 3D-2D pattern

ADMET (Absorption, Distribution, Metabolism, Elimination, and Toxicity)

Physicochemical Attributes

The top 5 ligand candidates were assessed using QikProp (Schrodinger Suite) for their physicochemical suitability. All compounds met acceptable criteria for molecular weight (≤ 669.091), hydrogen bond donors (≤ 3), and acceptors (≤ 6.8), suggesting good drug-likeness.

Pharmacokinetic Parameters

Human Oral Absorption (HOA) is a critical pharmacokinetic parameter during early drug development, reflecting a compound's potential for effective systemic exposure. In this study, all candidate ligands

displayed favorable HOA values ranging 100 %, suggesting good oral bioavailability and alignment with acceptable absorption criteria [34] (Table 3).

Aqueous solubility, an important factor influencing intestinal absorption and systemic distribution, was evaluated using the QPlogS descriptor. The solubility values obtained for the ligands ranged from -4.11 to -6.384, which are within the acceptable range for orally administered drugs (Table 3).

The QPPCaco descriptor was used to estimate intestinal permeability across the Caco-2 cell monolayer model, which serves as a proxy for gut-blood barrier penetration. Predicted permeability values ranged from 441.784 to 9906.038, indicating that the ligands possess sufficient capacity for intestinal absorption. Additionally, Protein binding affinity, particularly toward human serum albumin (HSA), was assessed via QPlogKhsa values. The results, which ranged from 0.182 to 0.828, fall within pharmacological acceptable thresholds, implying appropriate distribution behavior and limited risk of extensive protein binding that could compromise bioavailability (see Table 3)

Table 3: Determined ADME Properties using QikProp

Ligand Number	Physicochemical Properties				Pharmacokinetic Properties							Drug Likeness Properties		
	mol_MW	donorHB	acceptHB	QPlogS	HOA%	QPPCaco	QPlogKhsa	QPlogPw	QPlogBB	CNS	QPlogHERG	Rule Of Five	Rule Of Three	QPlogPo/w
D1	366.543	3	6.5	-5.099	100	441.784	0.182	9.478	-2.459	-2	-5.989	2	0	2.389
D2	669.085	3	3.4	-4.111	100	5630.075	0.654	5.981	0.339	-2	-2.703	2	0	2.902
D3	221.318	1	6.1	-6.144	100	9906.038	0.828	1.488	0.696	-2	-2.927	0	0	2.605
D4	360.492	1	5.7	-4.822	100	1171.148	0.574	7.926	-0.672	-2	-3.913	0	0	1.922
D5	350.579	0	5	-6.384	100	2594.031	0.5	3.64	-0.906	-1	-6.174	1	1	1.055

Drug-Likeness Evaluation

All selected ligands complied with Lipinski's Rule of Five and Jorgensen's Rule of Three, two widely accepted criteria for drug-likeness (Table 4). Their lipophilicity (QPlogPo/w) values ranged from 1.055 to 2.902. Synthetic accessibility score, computed using the QikProP platform, ranged from 1.54 to 2.24, indicating that these compounds are reasonably easy to synthesize [35, 36].

Table 4: Admissible ADME Data Set

S. No.	Descriptor	ADME Property	Permissible Ranges / Recommended Value
1	CNS	Predicted central nervous system activity on -2 to +2 scale	-2 (inactive) to +2 (active)
2	mol_MW	Molecular weight of the molecule	130 to 725
3	DHB	Estimated number of hydrogen bonds donated by solute in aqueous solution	0 to 6
4	AHB	Estimated number of hydrogen bonds accepted by solute in aqueous solution	2 to 20
5	QPPCaco	Predicted apparent Caco-2 cell permeability (nm/sec)	<25 = poor, >500 = great
6	QPlogPw	Predicted water/gas partition coefficient	4.0 - 45.0
7	QPlogPo/w	Predicted octanol/water partition coefficient	-2.0 - 6.5
8	QPlogS	Predicted aqueous solubility, log S in mol/dm ³	-6.5 - 0.5
9	QPlogKhsa	Predicted binding to human serum albumin	-1.5 - 1.5
10	QPlogHERG	Predicted IC ₅₀ for HERG K ⁺ channel blockage	Below +5.0
11	QPlogBB	Predicted blood/brain partition coefficient	-3.0 - 1.2
12	% Human Oral Absorption	Predicted human oral absorption on 0 to 100% scale	>80% = high; <25% = poor
13	Rule Of Five	Number of violations of Lipinski's Rule of Five	Maximum is 4
14	Rule Of Three	Number of violations of Jorgensen's Rule of Three	Maximum is 3
15	Synthetic Feasibility	Predicted synthetic feasibility on scale of 1 to 10	0 = high feasibility; 10 = least feasible
16	Lipophilicity	Predicted lipophilic nature of the ligand calculated from pIC ₅₀ - LogP	min -6; max +3

Toxicity Profiling

Toxicological evaluation focused on the potential of the ligands to inhibit Cytochrome P450 (CYP450) enzymes. Using Pro Tox 3.0 server, the compounds were classified as inhibitors or non – inhibitors of various CYP450 isoforms (Table 5), providing insight into possible drug interactions and metabolism [37, 38]. Overall, the ligands demonstrated strong ADMET characteristics, low toxicity, and feasible synthesis, highlighting their potential as therapeutic agents for cardiomyopathy.

Table 5: Overview of Toxicological properties

S. No.	CYP1A2	CYPC19	CYP2C9	CYP2D6	CYP3A4
D1	-Neg.	-Neg.	-Neg.	-Neg.	-Neg.
D2	-Neg.	-Neg.	-Neg.	-Neg.	-Neg.
D3	-Neg.	-Neg.	-Neg.	-Neg.	-Neg.
D4	-Neg.	-Neg.	-Neg.	-Neg.	-Neg.
D5	-Neg.	-Neg.	-Neg.	-Neg.	-Neg.

Table 5 illustrates the possible toxicological impact of ligands D1 to D5 on the cytochrome P450 enzyme. It explains whether each ligand, along with the cardiomyopathy drugs, functions as an inhibitor (+Pos. Values) and a non-inhibitor (-Neg. Values) of the P450 system.

CONCLUSION

This study presents a comprehensive computational approach to identify potential inhibitors targeting the TNNC1 protein, a critical regulator of myocardial contraction implicated in cardiomyopathy. Using structural bioinformatics tools, a reliable 3D model of TNNC1 was developed and validated through Ramachandran plot, ProSA, and VERIFY_3D analyses, ensuring stereochemical accuracy. Structure-based virtual screening of marine natural product libraries, followed by molecular docking via GLIDE, identified five ligands (D1–D5) with strong binding affinity and specific interactions with key residues such as ASP139 and ASP2. ADMET profiling revealed that all selected ligands exhibited favorable physicochemical properties, high oral absorption (HOA = 100%), suitable solubility (QlogS within -6.5 to 0.5), and acceptable permeability across the Caco-2 model. The ligands complied with Lipinski's Rule of Five and Jorgensen's Rule of Three, affirming their drug-likeness. Moreover, toxicity analysis through ProTox 3.0 confirmed that none of the compounds inhibit cytochrome P450 enzymes, indicating a low risk of metabolic interference or adverse effects. Overall, this study not only elucidates the structural and functional aspects of TNNC1 but also proposes novel lead compounds with strong inhibitory potential and favorable pharmacokinetics. These findings warrant further in vitro and in vivo investigations to validate their therapeutic efficacy against cardiomyopathy.

REFERENCES

1. Landstrom, A. P., Parvatiyar, M. S., Pinto, J. R., Marquardt, M. L., Bos, J. M., Tester, D. J., Potter, J. D., & Ackerman, M. J. (2008). Molecular and functional characterization of novel hypertrophic cardiomyopathy susceptibility mutations in TNNC1-encoded troponin C (A8V, C84Y, E134D, D145E). *Journal of Molecular and Cellular Cardiology*, 45(2), 281–288.
2. Milburn, G. N. (2025). Biochemical and biophysical properties of failing myocardium in rare patient populations. University of Kentucky Theses and Dissertations. https://uknowledge.uky.edu/physiology_etds/71
3. Landstrom, A. P., Parvatiyar, M. S., & Ackerman, M. J. (2008). Mutations in the cardiac troponin C gene are associated with dilated cardiomyopathy. *Journal of Clinical Investigation*, 118(10), 4091–4101. <https://doi.org/10.1172/JCI36162>
4. Functional Analysis of a Unique Troponin C Mutation, Gly159Asp, that Causes Familial Dilated Cardiomyopathy, Studied in Explanted Heart Muscle (2008). *Circulation: Heart Failure*.
5. Wang, X., Solaro, R. J., & Dong, W. J. (2025). Myosin–actin crossbridge-independent sarcomere length–induced Ca²⁺ sensitivity changes in skinned myocardial fibers: Role of myosin heads. *Journal of Molecular and Cellular Cardiology*. <https://doi.org/10.1016/j.yjmcc.2025.02.005>
6. Pinto, J. R., Parvatiyar, M. S., Jones, M. A., Liang, J., Ackerman, M. J., & Potter, J. D. (2009). A functional and structural study of troponin C mutations related to hypertrophic cardiomyopathy. *Journal of Biological Chemistry*, 284(28), 19090–19100.
7. Severe disease expression of cardiac troponin C and T mutations in idiopathic dilated cardiomyopathy. (2004). *Journal of the American College of Cardiology*, 43(9), 1713–1719.
8. Li, M. X., & Hwang, P. M. (2015). Structure and function of cardiac troponin C (TNNC1): Implications for heart failure, cardiomyopathies, and troponin modulating drugs. *Gene*, 571(2), 153–166. <https://doi.org/10.1016/j.gene.2015.06.063>.

9. Gomes, A. V., Pinto, J. R., & Szczesna-Cordary, D. (2025). Physiology of human myopathies: Effects of the TNNC1 G159D mutation on cardiac structure and function. *Frontiers in Physiology*, 16, Article 1597211.
10. Thin filament cardiomyopathies review: TNNC1 mutations in HCM/DCM & prognosis (~1% of HCM cases; de novo/death risk). (2022). *Frontiers in Cardiovascular Medicine*.
11. Functional Analysis of a Unique Troponin C Mutation, Gly159Asp, that Causes Familial Dilated Cardiomyopathy, Studied in Explanted Heart Muscle (2008). *Circulation: Heart Failure*.
12. The UniProt Consortium. (2023). UniProt: the Universal Protein Knowledgebase in 2023. *Nucleic Acids Research*, 51(D1), D523–D531. <https://doi.org/10.1093/nar/gkac1052>
13. Burley, S. K., Berman, H. M., Bhikadiya, C., Bi, C., Chen, L., et al. (2021). RCSB Protein Data Bank: Powerful new tools for exploring 3D structures of biological macromolecules for basic and applied research and education. *Nucleic Acids Research*, 49(D1), D437–D451. <https://doi.org/10.1093/nar/gkaa1038>
14. Laskowski, R. A., MacArthur, M. W., Moss, D. S., & Thornton, J. M. (1993). PROCHECK: A program to check the stereochemical quality of protein structures. *Journal of Applied Crystallography*, 26(2), 283–291. <https://doi.org/10.1107/S0021889892009944>
15. R Dumpati, V Ramatenki, R Vadija, S Vellanki, U Vuruputuri. (2018). Structural insights into suppressor of cytokine signaling 1 protein-identification of new leads for type 2 diabetes mellitus, *Journal of Molecular Recognition* 31 (7), e2706
16. R Dumpati, R Dulapalli, B Kondagari, V Ramatenki, S Vellanki, R Vadija. (2016). Suppressor of cytokine signalling-3 as a drug target for type 2 diabetes mellitus: a structure-guided approach, *ChemistrySelect* 1 (10), 2502-2514
17. Muddagoni et al. (2021): Homology modeling validated with ProSA and Verify3D; binding-site identification via SiteMap; virtual screening using Schrödinger suite (LigPrep → Glide docking → QikProp ADME profiling)
18. Bhargavi, M., & Bhargavi, S. G. (2025). Computational approach for HDAC1 predicting protein-ligand interactions for cancer through homology modelling, virtual screening and molecular docking. *Shanlax Publications – Computational Technology & Biology*. <https://www.shanlaxpublications.com/p/ctbtls/ch002.pdf>
19. Sastry, G. M., Adzhigirey, M., Day, T., Annabhimoju, R., & Sherman, W. (2013). Protein and ligand preparation: Parameters, protocols, and influence on virtual screening enrichments. *Journal of Computer-Aided Molecular Design*, 27(3), 221–234.
20. Rocca, R., Alcaro, S., & Artese, A. (2024). Structure-based virtual screening and molecular dynamics simulations of FDA-approved drugs targeting MALAT1. *Med Chem Res* 33, 2095–2100. <https://doi.org/10.1007/s00044-024-03336-7>
21. Friesner, R. A., Banks, J. L., Murphy, R. B., Halgren, T. A., et al. (2004). Glide: A new approach for rapid, accurate docking and scoring. 1. Method and assessment of docking accuracy. *Journal of Medicinal Chemistry*, 47(7), 1739–1749. <https://doi.org/10.1021/jm0306430>
22. Afendi, F. M., Okada, T., Yamazaki, M., Hirai-Morita, A., Nakamura, Y., Nakamura, K., ... & Saito, K. (2020). CMNPD: A comprehensive marine natural products database towards facilitating drug discovery from the ocean. *Nucleic Acids Research*, 48(D1), D509–D516. <https://doi.org/10.1093/nar/gkz890>
23. Schrödinger, LLC. (2024). Schrödinger Suite, Release 2024-1. New York, NY: Schrödinger, LLC. Retrieved from <https://www.schrodinger.com>
24. Ibrahim, Z. Y., Abdulfatai, U., Ejeh, S., Ajala, A., & Adawara, S. N. (2024). QSAR and ADMET screening to assess antimalarial potential of Amodiaquine derivatives. *The Microbe*. <https://doi.org/10.1016/j.microb.2024.100208>
25. Jamal, S., Goyal, S., Shanker, A., & Grover, A. (2015). Computational study of glutamate receptor modulation for cognitive dysfunction using Glide. *PLOS ONE*, 10(5), e0129370. <https://doi.org/10.1371/journal.pone.0129370>
26. Mishra, S., & Subbarao, N. (2022). Docking and simulation of SARS-CoV-2 Mpro inhibitors using Glide and FEP. *Computers in Biology and Medicine*, 145, 105408. <https://doi.org/10.1016/j.combiomed.2022.105408>
27. Wiederstein M & Sippl MJ (2007) ProSA-web: interactive web service for the recognition of errors in three-dimensional structures of proteins. *Nucleic Acids Res* 35, W407–W410
28. Tian, W., et al. (2018). CASTp 3.0: computed atlas of surface topography of proteins. *Nucleic Acids Res*, 46(W1), W363–W367. <https://doi.org/10.1093/nar/gky473>
29. Basnet, S., Ghimire, M. P., Lamichhane, T. R., & Adhikari, R. (2023). Identification of potential human pancreatic α -amylase inhibitors from natural products by molecular docking, MM/GBSA calculations, MD simulations, and ADMET prediction. *PLOS ONE*, 18(9), e0275765. <https://doi.org/10.1371/journal.pone.0275765>
30. Dhameliya, T. M., Nagar, P. R., & Gajjar, N. D. (2022). Systematic virtual screening in search of SARS CoV-2 inhibitors against spike glycoprotein: pharmacophore screening, molecular docking, ADMET analysis, and molecular dynamics. *Molecular Diversity*, 26, 1351–1370.
31. Cheng, T., Li, Q., Zhou, Z., Wang, Y., & Bryant, S. H. (2012). structure-based virtual screening for drug discovery: a problem-centric review. *AAPS Journal*, 14(1), 133–141.
32. BIOVIA, Dassault Systèmes. (2020). *Discovery Studio Modeling Environment*, Release 2020. San Diego, CA: Dassault Systèmes.
33. Banerjee, P., et al. (2018). ProTox-II: prediction of toxicity of chemicals. *Nucleic Acids Res*, 46(W1), W257–W263. <https://doi.org/10.1093/nar/gky318>
34. Drwal, M. N., Banerjee, P., Dunkel, M., Wettig, M. R., & Preissner, R. (2014). ProTox: a web server for the in silico prediction of rodent oral toxicity. *Nucleic Acids Research*, 42(W1), W53–W58.

35. Lipinski, C. A., Lombardo, F., Dominy, B. W., & Feeney, P. J. (2001). Experimental and computational approaches to estimate solubility and permeability in drug discovery and development settings. *Advanced Drug Delivery Reviews*, 46(1-3), 3-26
36. Batool, M., Ahmad, B., & Choi, S. (2019). A structure-based drug discovery paradigm. *International Journal of Molecular Sciences*, 20(11), 2783.
37. Ambatkar, M. P., Rarokar, N. R., & Khedekar, P. B. (2024). Study of Some Substituted Quinolines as TRPV1 Inhibitors by In Silico and In Vivo Methods. *Pharmaceutical Chemistry Journal*. <https://doi.org/10.1007/s11094-024-03244-5>

Copyright: © 2025 Author. This is an open access article distributed under the Creative Commons Attribution License, which permits unrestricted use, distribution, and reproduction in any medium, provided the original work is properly cited.